Enhancing Tensile Strength of FDM parts using Thermal Annealing and Uniaxial Pressure

by

RHUGDHRIVYA RANE

Presented to the Faculty of the Graduate School of

The University of Texas at Arlington in Partial Fulfillment

of the Requirements

for the Degree of

MASTER OF SCIENCE IN MECHANICAL ENGINEERING

THE UNIVERSITY OF TEXAS AT ARLINGTON

December 2018

Acknowledgements

I would firstly like to thank Dr. Robert Taylor for mentoring and guiding me throughout my coursework and being a constant source of motivation. I would also like to thank Dr. Ankur Jain and Dr. Ashfaq Adnan for not only providing me with their valuable feedback but also for allowing me to use their lab equipment as and when necessary.

I would like to thank Mr. Hardik Jain for helping me to obtain the cross-sectional images of the test parts. I am deeply thankful to Mr. Sangram Advirkar for helping me to print the test parts. I would like to extend my gratitude to my parents for being supportive of my academic pursuits. I would especially like to dedicate this work to my mother, Anjana, as none of this would be possible without her.

December 5, 2018

Abstract

Enhancing Tensile Strength of FDM parts using Thermal Annealing and Uniaxial Pressure

Rhugdhrivya Rane, MS

The University of Texas at Arlington, 2018

Supervising Professor: Robert Taylor

Additive manufacturing has been a revolutionary and disruptive technological development in the field of design and manufacturing with Fused deposition modelling (FDM) being at the forefront of this technology. But it is seen that parts printed using FDM suffer from an inherent deficiency of weak tensile strength in the out of plane direction (z-direction) thus limiting their application. This issue of weak z-direction strength is due to the weak Inter-bead bond strength of adjacent polymer interfaces. The purpose of this work is to increase this Inter-Bead bond strength thus increasing the overall tensile strength of the part. In this work, FDM was used to print tensile specimens made of Acrylonitrile Butadiene Styrene (ABS), which were subjected to varying values of isothermal heating and uniaxial pressure which was along the z-direction. Multiple values of temperature and pressure were chosen to investigate their effect of the deformation of the part and

try to maintain geometric accuracy. The thermally annealed parts were then subjected to tensile loading to check the increase in strength. It was seen that when the parts were subjected to only thermal annealing there was a slight increase in the tensile strength of the part. But when the parts were subjected to a combination isothermal heating and pressure the increase in strength was considerably more as compared to only thermal annealing for the same time period. A cross sectional view of the layer to layer bonding was studied under the microscope which showed a change in the mesostructure of the part. From previous studies it had been seen that when two polymer interfaces have intimate contact while undergoing thermal annealing above the glass transition temperature Reptation occurred. This theory of Reptation was seen to be the reason for the considerable increase in strength and lead changes in the mesostructure of the part. The investigations done in this study provide ground work to increase the total structural strength of the parts with a special focus on the inter laminar bonding which affects the z-direction strength.

TABLE OF CONTENTS

List of Illustrations

List of Tables

Chapter 1 Introduction

Additive manufacturing (AM) is a disruptive manufacturing technique as it enables fabrication of complex part geometries which were previously considered difficult to manufacture using conventional methods. AM has gained popularity due to its low cost, low production capability to print highly complex and customizable parts with a multitude of materials. Fused Deposition Modeling (FDM) is one of the most commonly used additive manufacturing technologies in terms of number of parts produced, printers, and printer manufacturers worldwide [1]. But parts fabricated using FDM cannot be used for most engineering applications due to their insufficient and anisotropic mechanical properties especially in the out of plane (z-plane) direction. This deficiency in mechanical properties is due to the weak Inter-laminar bonding in the adjacent layers of FDM parts leading to an overall reduction in part strength [1]. Thus, to enhance the use of FDM parts in actual engineering application and not just artistic renderings, the overall anisotropy of the parts has to be reduced while increasing the strength.

The aim of this study is to investigate the increase in tensile strength of the FDM parts by the application of post processes such as: 1) thermal annealing and 2) thermal annealing accompanied with a unidirectional mechanical pressure in the Z- direction. The increase in the bond length and its corresponding effect on the tensile strength is also studied to provide a better understanding regarding the

increase in strength. Therefore, we experimentally tried to investigate the effect of the combinations of the above given parameters on the tensile strength.

Chapter 2 Background

2.1 Additive Manufacturing

Manufacturing techniques have constantly been evolving to better accommodate the manufacturing of complex and dimensionally accurate parts. Additive Manufacturing (AM) was one such technique which allowed for the fabrication of complex geometries with relative ease. In AM, a computer-generated model is used to fabricate the part in layer by layer fashion using either metal powder or plastic feedstock. AM uses digital technology to build the printed part rather than using the traditional mold manufacturing, which involves complex designing and is time consuming [2]. Unlike conventional subtractive manufacturing methods where material is machined away to obtain the desired geometries and then assembled to form the final product, AM only adds material layer by layer to build the desired part. This not only reduces the amount of material wasted and the assembly time but also provides the freedom to manufacture far more complex geometries. AM has accentuated the freedom of designing and fabricating parts because internal features and complex, previously non-viable geometries can easily be fabricated using AM [3].

The AM processes have been divided into seven categories by the ASTM F42 committee in an attempt to standardize the terminology [4]. These processes vary from one another based on the method of material deposition, the energy

source used, and the state of the build material used (wire feedstock, liquid, powder or sheets). These processes are listed as follows:

1) Binder jetting: A liquid bonding agent is selectively deposited to join powder materials.

2) Directed energy deposition: Focused thermal energy (Laser, Electron beam or Plasma) is used to fuse materials by melting as they are being deposited.

3) Material extrusion: Filament is selectively dispensed through a heated nozzle or orifice.

4) Material jetting: Droplets of build material such as photopolymer or wax are selectively deposited.

5) Powder bed fusion: Thermal energy is used to selectively fuse regions of a powder bed. Powders may be metals or polymers.

6) Sheet lamination: Sheets of material are bonded to form an object.

7) Vat photopolymerization: Liquid photopolymer in a vat is selectively cured by light-activated polymerization. One or more lasers are used as the energy source to cure the photopolymer.

2.2 Fused Deposition Modeling

Fused deposition modeling (FDM) or Fused Filament Modeling (FFF) is one of the most popular and rapidly growing AM technologies with growing application in finished part manufacturing [1]. FDM was known as rapid prototyping technology as it involved printing rudimentary 3D designs for visual aid or presentation [5]. But recently there has been an increase in the use of FDM to manufacture finished parts [1]. The popularity of FDM is also due to its comparatively low costs and simple feedstock to other AM technologies [6].

2.2.1 Operation

FDM systems build 3D objects layer by layer from a CAD design. In FDM, a filament of thermoplastic material is forced through a heated liquefier with the help of a pinch roller. A gantry moves the print nozzle in the horizontal x-y direction while depositing the material on the build surface [1]. The three-axis movement is completed by either the bed moving downwards or the nozzle head moving upwards by a distance equal to that of the specified layer height. Nozzles diameters can vary from 0.010 to 0.05 in [7]. A continuous positive force required for extrusion is provided by the rollers driving the incoming filament [7]. This filament fed into the liquefier melts and the solid portion of the filament acts as a piston pushing the melt through the nozzle [1].

2.2.2 Materials

FDM works best with polymers that are amorphous in nature rather than highly crystalline polymers. This is because in FDM the extrusion takes place in the form of a viscous paste. As amorphous polymers do not have a distinct melting point but rather the viscosity lowers with increasing temperature. Thus, the viscosity at which the amorphous polymers can be extruded is high enough for it to maintain the extruded shape and solidify quickly. Also, when material is added in an adjacent road or as a new layer it can bond easily with the previously extruded material [5].

The most common amorphous polymer used in FDM is Acrylonitrile Butadiene Styrene (ABS). ABSplus material is the updated version of ABS which is commercially available. Also, Stratasys provides its own blends of ABS namely ABS-M30 (stronger and tougher than standard ABS) and ABS-M30i (Biocompatible material) [8]. The ABSi material provides a translucent effect with properties similar to ABS.

In applications where ABS cannot fulfill the requirements a PC- based material, formulated to ISO 10993-1 and USP Class VI requirements, is used. ULTEM 9085 is another material that has been developed with favorable flame, smoke and toxicity (FST) ratings and thus is suitable for use in aerospace and marine applications. Polyphenylsulphone (PPSF) is another sophisticated material which can be used in applications that require improved heat deflection [5].

2.3 Parameters Affecting strength of FDM parts

Apart from the strength of the bulk material used, the overall strength of FDM parts is largely affected by the various printing and slicing parameters. The effect of the parameters on strength have been discussed in the upcoming sections. These parameters play a crucial role in this study as they provide us with the means to compare and test the effect of the post printing thermal annealing and uniaxial pressure on parts printed with optimal print settings and parts printed with below par print settings.

2.3.1 Infill Percentage

Infill refers to the amount of material required to build the part. Infill percentage is the percentage value of the amount of material used to manufacture the part with respect to the volume of the part. As infill percentage increases the part becomes heavier and denser. Thus, infill percentage directly correlates to part strength, as infill percentage goes up the parts exhibit higher values of stiffness and strength.

2.3.2 Infill Pattern

Various infill patterns are available for parts printed in FDM. These can be broadly classified as Rectilinear, Diagonal, Hexagonal, Honeycomb, Hexagonal etc. Some of these can be seen in Figure 1.

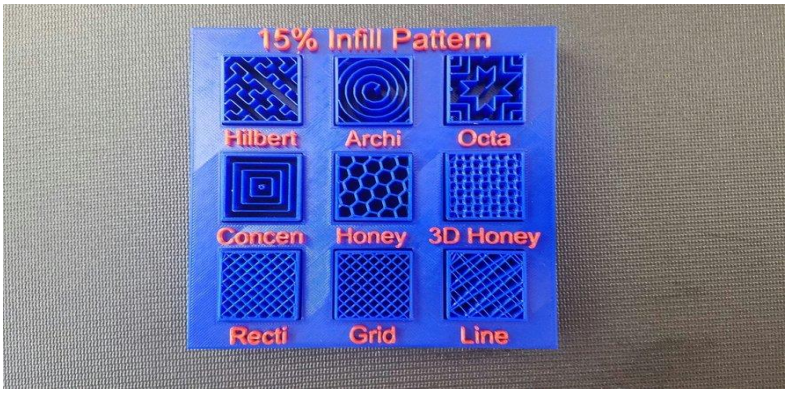

Figure 1: Different infill patterns used in FDM [9].

2.3.3 Number of Perimeter Shells

Perimeter shells are loops formed around the internal raster by the extruder as shown in Figure 2. The number of perimeter shells can be specified in the slicer by the user. An increase in the number of shells for printed tends to increase total strength of the part.

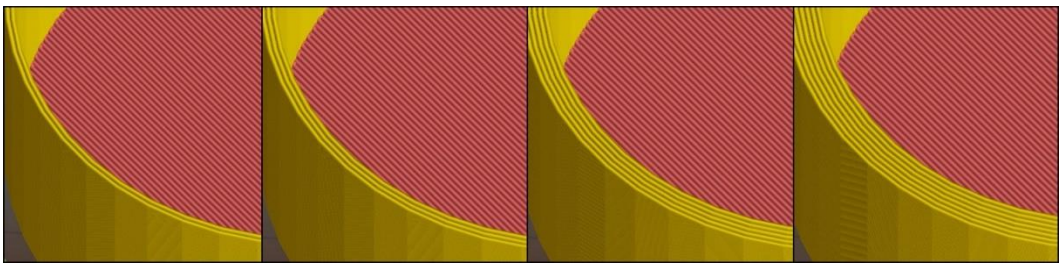

Figure 2: Parts printed using varying numbers of perimeter shells [10].

2.3.4 Print Orientation

FDM parts can be printed using different plane orientations. The orientation of the printed part dictates the mechanical strength of the parts. Parts printed using FDM are the weakest when loaded along the Z- direction (Out of plane). This results in anisotropic properties of FDM parts. Thus, to get optimized strength the orientation of the print should be in such a way that the direction of loading should not coincide with the build direction.

2.3.5 Layer Height

FDM parts are built in a layer wise fashion by extruding one layer on top of the other. The layer height affects the surface finish of the part and can be modified in the slicer. Though smaller layer heights lead to a better surface finishes there is a trade-off between the layer height and the amount of print time needed, decreasing the layer height leads to larger print times.

2.3.6 Flow Rate

Flow rate of the extruded material through the nozzle has a significant effect on the total strength of the parts. As the flow rate increases the mesostructure of the FDM parts is affected leading to a decrease in the size of the voids and an increase in the contact area between adjacent layers. This leads to considerably larger values of ultimate tensile strength for parts printed with higher flow rates.

2.4 Mechanical Properties of FDM Parts

Though FDM is one of the most popular AM technologies due to its low cost of operation and comparatively cheap feedstock it has many limitations to it. The mechanical properties of the parts fabricated using FDM largely depend on the material, processing and geometric details [11]. It is seen that the mechanical properties of these parts are affected by various print parameters like build orientation [12], layer thickness [13,14], air gap [15,16] and printing temperatures [17], leading to orthotropic properties. One of the major limitations is that parts fabricated using FDM fail to match the mechanical properties exhibited by similar parts manufactured using conventional manufacturing techniques (injection molding). This depreciation in mechanical properties is due to two primary factors: porosity and imperfect weld-lines [18]. As FDM uses circular nozzles to print parts. the rounded features of the deposited polymer melt do not stack perfectly leading to inherent porosity [19]. Also, long void spaces are present, both within a build plane and between planes. Thus, even when there is intimate contact between the polymer traces the interface strength is not comparable to that of the bulk polymer [18]. The interfaces are formed when molten polymer is extruded onto previously deposited polymer melt which has cooled down to a lower temperature. These interfaces act as points of failure initiations giving FDM parts orthotropic properties. Therefore, parts printed using FDM are inherently highly anisotropic in nature with the weakest loading direction being in the out of plane or Z-direction.

The interlaminar bond-forming processes can be improved by using higher temperature and lower deposition rates, but these changes lead to poorer geometric control, lower surface quality and longer print times [18]. For FDM parts to be used as final use parts their mechanical properties need to be drastically improved and should be comparable with that of the bulk material.

2.5 Bond Formation and Strength

In ideal conditions a bond can be formed by bringing the surfaces as close as the equilibrium spacing of the atoms such that the attractive and repulsive forces of the surface molecules are balanced. The net potential energy of such a system is at a minimum and is equal to the energy with which the atoms are bonded. But due to surface asperities and the complex nature of polymer molecules, only one in a billion atoms forms such a bond along a real surface. Thus, the joint strength is only one-billionth of the theoretical strength that can be achieved [20]. Thus, to enhance a joint strength application of heat and pressure are the critical factors. In FDM, the formation of bonds among the polymer filaments is driven by the thermal energy of the polymer filaments. The temperature history plays a major role in the bond quality formed which in turn affect the mechanical properties of the part. The growth of the neck formed between the two adjacent filaments and the thermal healing are the major factors affecting the bond quality. The sequential stages of

bond formation in FDM parts can be seen in Figure 3. In Figure 3 the cross sections of the filaments have been idealized as circles [17].

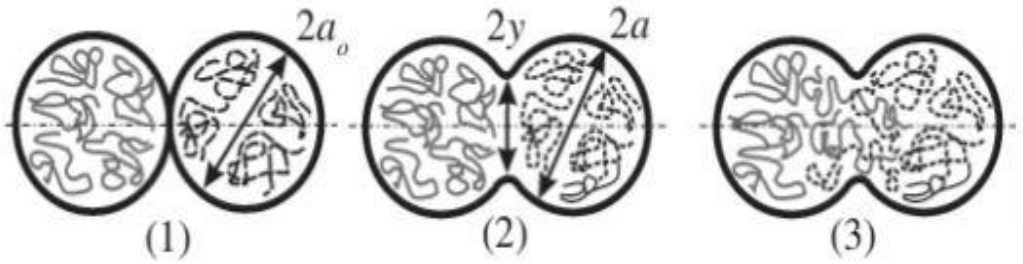

Figure 3: Stages of bond formation in FDM [17].

The dimensionless sintering neck growth is calculated as the ratio of neck radius "y" with filaments radius "a" as shown in Figure 3.

There are four critical sequential stages which can summarize the melt-bonding process of thermoplastic interfaces [21]:

1) Interface Heating, this enables local polymer flow and molecular mobility.
2) Intimate contact, or close physical contact between the two interfaces.
3) Molecular diffusion (thermal healing) and randomization across interfaces.
4) Polymer cooling below glass transition temperature (T_g).

Intimate contact and thermal healing are two important governing mechanisms affecting thermal fusion bonding. These have been discussed in detail in the further sections.

2.5.1 Intimate Contact

Intimate contact represents the amount of physical area contact that has been established between two surfaces after they are brought in contact [22]. This intimate contact is affected because of the presence of surface asperities as no materials have perfectly smooth surfaces. Due to these asperities perfect contact is not established, and the total contact area is reduced. But when heat and pressure are applied the surface asperities start to deform and there is an increase in the total contact area of the surfaces. As thermoplastics have temperature dependent viscosity an increase in temperature facilitates the flow, allowing for greater contact.

Degree of intimate contact ($D_{ic)}$ is defined as the fraction of the total surface area that is in contact. D_{ic} is a function of various factors such as applied temperature and pressure, duration of application, and a surface roughness parameter characterizing asperities. A model was developed by Dara and Loos to describe the intimate contact between the surfaces. In their model they assumed the asperities along the imperfect surface to be in the form of a wave made up of rectangular elements of varying sizes. This model was further developed by Lee and Springer. In the Lee-Springer model the rectangular elements were idealized to be identically sized and the dependence of intimate contact on applied pressure and temperature-dependent viscosity was shown. The same model was developed by Mantell and Springer to accommodate for time-varying properties and thus explain

intimate contact. In the Mantell-Springer model the applied force is assumed to cause deformation of the rectangular elements thus leading to an increase in area of contact. In this work we investigate the effect of increase in inter-laminar bond strength due to a uniaxial pressure which leads to an increase in intimate contact.

2.5.2 Thermoplastic Healing

FDM parts built with rasters oriented at bias angles to the primary axis of the structure morphologically resemble laminated composite materials. Each layer of FDM parts can be treated as a composite lamina with anisotropic strength and stiffness [23]. Therefore, the interlaminar bond formation in FDM parts is like that as seen in composite structures and occurs due to the phenomenon of thermoplastic healing. When two thermoplastics are brought into good contact above the glass transition temperature, the interface starts to gradually disappear and the mechanical strength at the interface starts to develop due to thermoplastic or crack healing [21]. This thermoplastic healing is primarily a result of polymer chain diffusion across the interface. This chain diffusion can be explained using the Reptation theory proposed by de Gennes.

2.5.3 Reptation Theory of Chain Mobility

To describe the thermal or crack healing due to polymer chain motion and entanglement the Reptation model provided by de Gennes is suitable. According to the reptation model the constraints imposed on a chain due to entanglements of the chain confine the chain inside a tube-like region [24, 25]. During thermal fluctuations the chain starts wriggling around in the tube. de Gennes said that the wriggling occurred rapidly with small magnitudes. According to the reptation model for time scales greater than that of the wriggling motion the polymer chain moves back and forth along the center line of the tube keeping the arc length constant. The conformation of the chain at any particular moment is the same as that of the tube confining it. Therefore, for a polymer chain to change its conformation it needs to break itself away from the tube that confines it. Figure 4 shows the disengagements of the chain from its initial tube that constrains its motion.

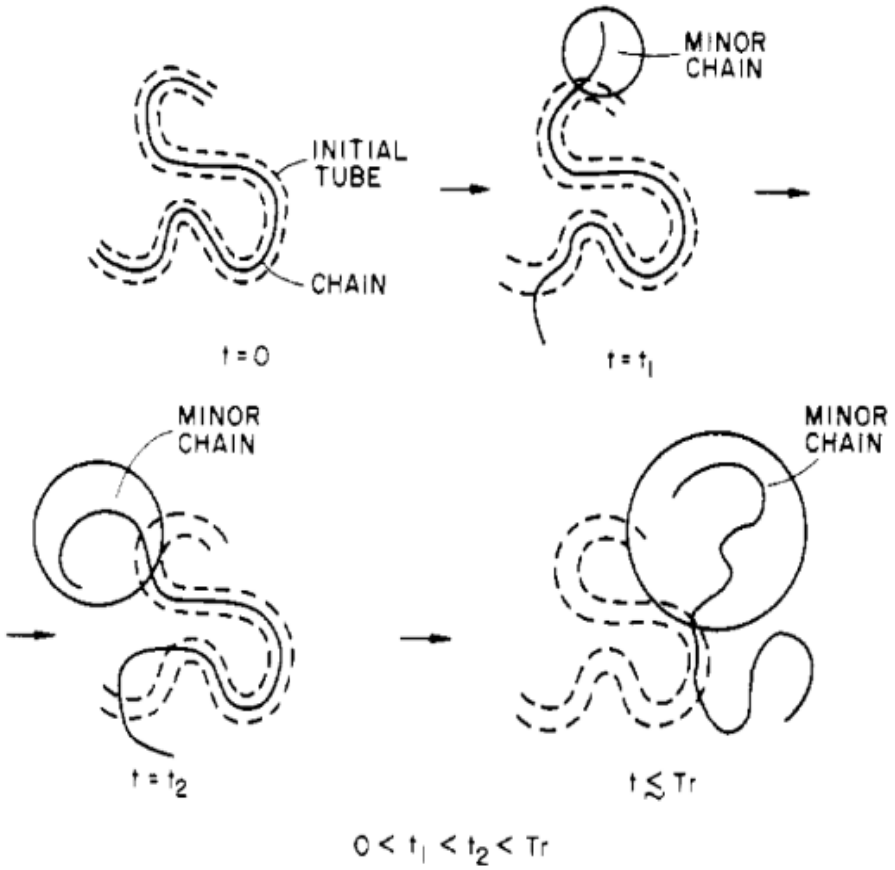

Figure 4: Temporal disengagement of polymer chains from the initial tube [21].

The part of the chain that have managed to escape from the initial tube and are no longer inside it are referred to as minor chains. The length of the minor chains is a function of time as shown in Figure 5.

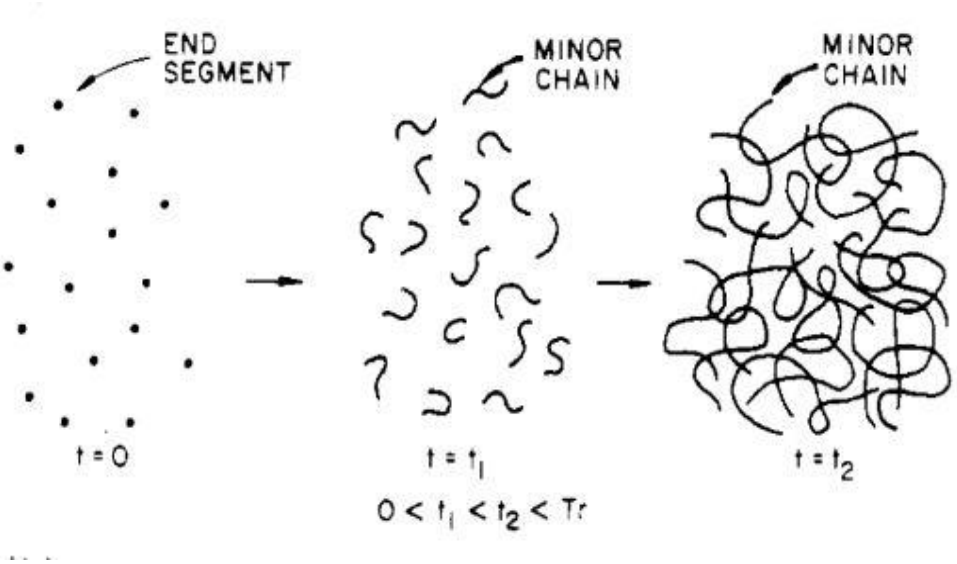

Figure 5: Minor chains at different times [21].

The minor chains have lost the memory of their initial conformations and as their length increases the initial conformations are replaced by new ones. But as the chain is in a dense system it is always in a new tube but only parts of the chain (central portions) retain some memory of the initial tube conformation. The two important time scales associated with the reptation model are T_e, or the time associated with the short- range wriggling motion and T_r, the amount of time required for the chain to completely disengage itself from the tube. Minor chains play an important role when describing the chain motion at a polymer-polymer interface. The chain conformation at a polymer- polymer interface before and after diffusion is shown in Figure 6.

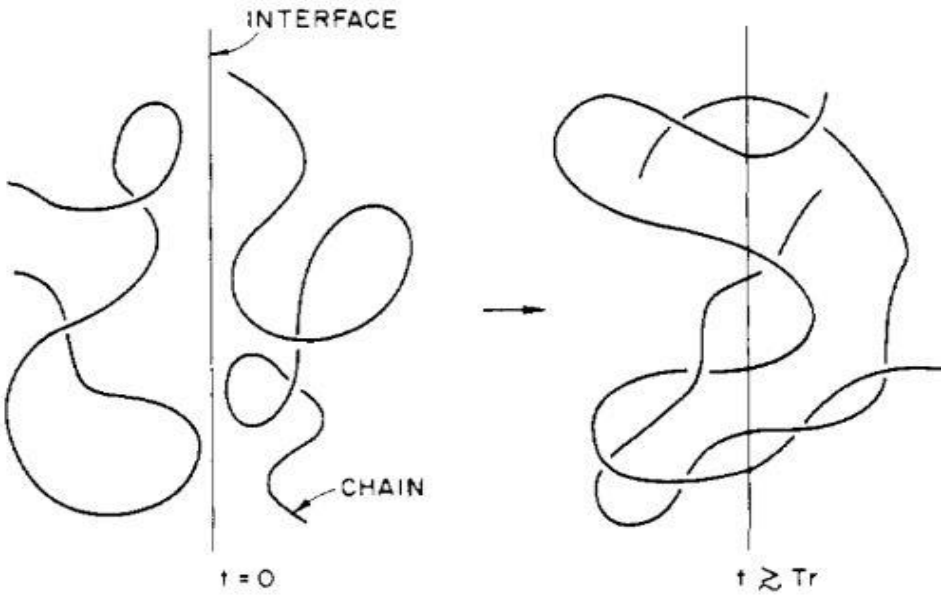

Figure 6: Conformation of chains at the interface before and after diffusion [21].

When we consider the motion of a single chain at the interface from the point of reptation model we see that initially the chain has conformations same as that of the initial tube. But as time progresses minor chains escape from this initial tube and new conformations are formed. These minor chains may assume any conformation and may also cross the interface. As time progresses the length of the minor chains increases, and these may cross the polymer-polymer interface multiple times and penetrate more deeply into the other side as seen in Figure 7. It is seen that only minor chains can cross the interface. The growth and random Gaussian conformations of minor chains constitute the diffusion and randomization of chains across the interface [21].

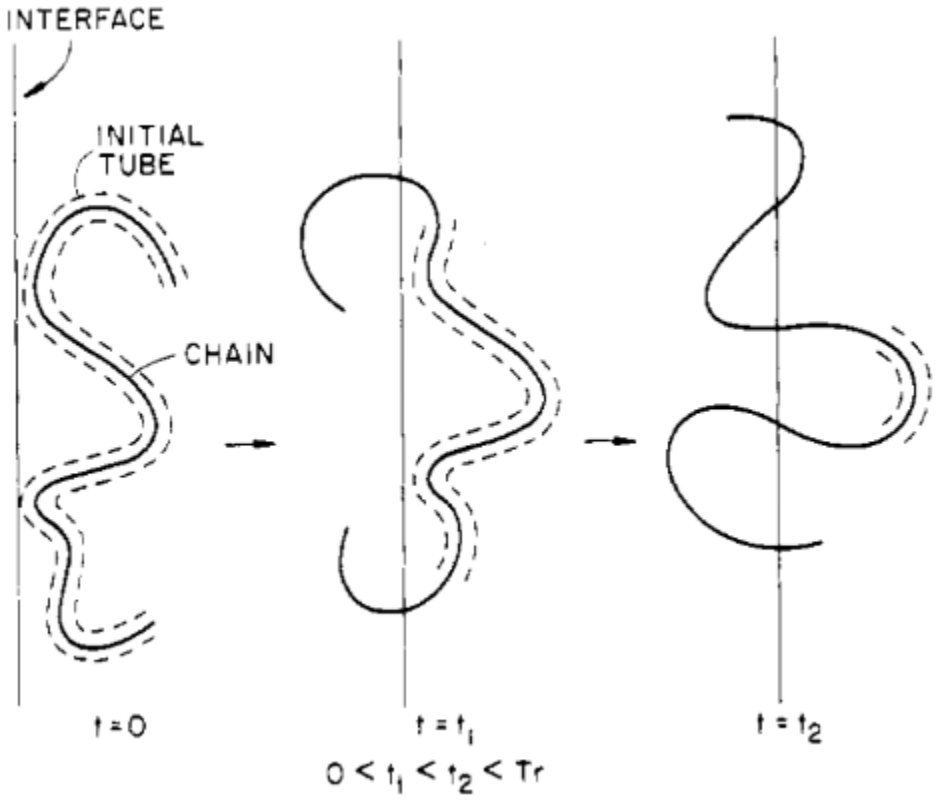

Figure 7: Disengagement of chain from the initial tube near an interface [21].

The time required to achieve complete healing across the interface is called molecular relaxation time or reptation time. According to reptation theory the average interpenetration distance of the chain ends across the interface (X) is given by:

$$X \propto \left(\frac{t}{M}\right)^{\frac{1}{4}}$$

This equation relates the interpenetration distance of chain molecules to time and molecular weight of the polymers. It is seen that as time increases the interpenetration distance of the chain ends across the interface increases. It was shown by Kim and Wool [21] that strength development is proportional to the average interpenetration distance of the polymers across the interface.

$$\sigma \propto X$$

$$\sigma \propto \left(\frac{t}{M}\right)^{\frac{1}{4}}$$

Thus, it is seen that the strength development is dependent on time and molecular weight for the monodisperse systems. As the time approaches reptation time, diffusion and randomization stages are complete and the full potential strength of the bond is reached, σ_{∞}.

$$\sigma_{\infty} \propto \left(\frac{t_r}{M}\right)^{\frac{1}{4}}$$

Where,

t_r = Reptation time or relaxation time at a given temperature

Reptation time is also the time required to obtain full healing at the interface. Degree of healing ($D_{h)}$ can be defined as the maximum obtainable strength after a certain time [22]. Degree of healing can be represented as the ratio of actual bondline strength to the maximum realizable strength of the material.

$$D_h = \frac{\sigma}{\sigma_\infty}$$

Therefore, by combining equation the above equations we get,

$$D_h = \left(\frac{t}{t_r}\right)^{\frac{1}{4}}$$

From the above equation we can see the time dependence of strength buildup. The cohesive strength is said to be reached when the two interfaces are indistinguishable.

2.6 Effect of Temperature on Viscosity of Amorphous Polymers

The polymer melt viscosity is affected by several factors such as temperature, pressure, molecular characteristics and addition of fillers. But it is seen that temperature has the most significant impact on the flow properties of polymer melts. It is seen that as the temperature increases beyond the glass transition temperature the viscosity of the polymers decreases leading to increased flow.

Chapter 3 Methodology

To test the increase in strength of the parts a custom test specimen was designed, and a fixture was built to accommodate the test specimens during heat treatment and prevent distortion allowing the specimens to maintain their original geometries. The parts were printed using two different sets of print parameters: high and low settings, to investigate the effect of heat treatment on both sets of print parameters. The values of temperature, time and applied pressure during heat treatment were varied to obtain a detailed comparative study and the correlation between the given variables and the increase in ultimate tensile strength. A cross-sectional view of the parts was obtained under a microscope to study the changes in the mesostructure of the parts after the post processing. This provides us with the means to explain the increase in the strength based on visible physical changes in the mesostructured.

3.1 Test Specimens Design

The specimens were designed on Solidworks using a modified version of ASTM D638-02a standards as shown in Figure 8. The dimensions of the dogbone specimen were scaled down to reduce print time of each part. The final design was saved as a .STL file format which was later used as the input for the slicing software.

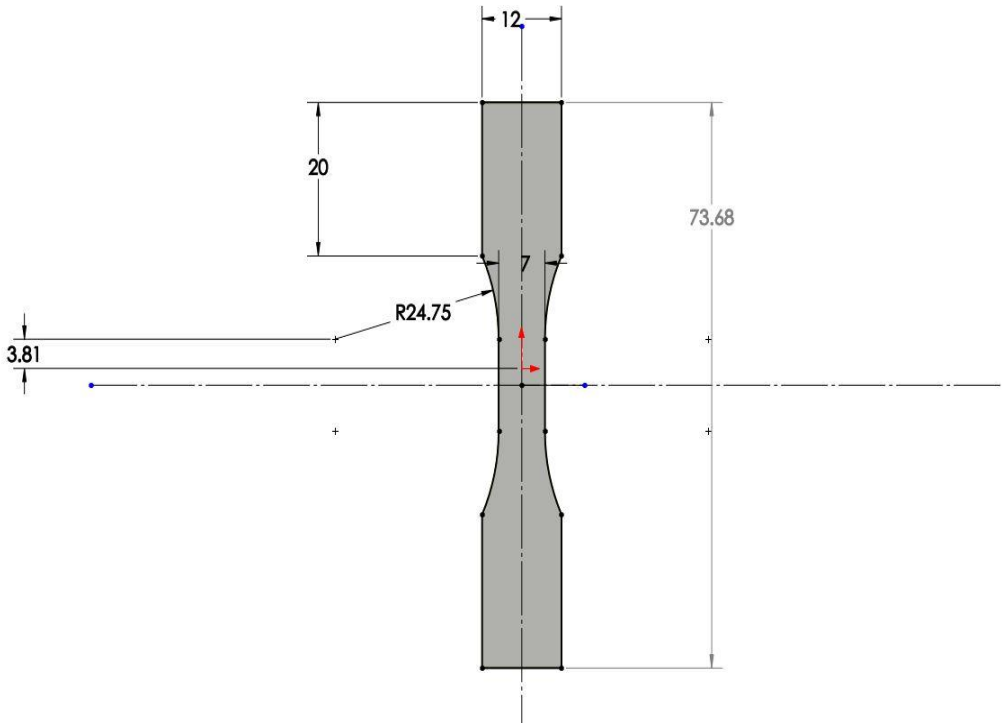

Figure 8: Tensile test specimen with modified geometry.

3.2 Print Parameters and Dogbone Fabrication

The test specimen was sliced using Simplify 3D and printed on Polyprinter 229. The specimens were printed using Acrylonitrile Butadiene Styrene (ABS) filament of 1.75mm diameter. Two combinations of print parameters were used, the details of the which are given in Table 1.

Table 1: Print Parameters used to print the dogbone specimens.

Print Parameters	Set 1: High settings	Set 2: Low settings
Extrusion Multiplier	1.2	0.8
Number of perimeter shells	2	1
Layer Height	0.2 mm	0.3 mm
Extrusion Temperature	230 °C	225 °C
Print speed	3600 mm/min	4500 mm/min
Total Print Time per specimen	1 hour and 3 minutes	33 minutes
Raster Angle	0°	0°

Extrusion multiplier allows to change the flow rate of the material from the nozzle. The specimens were printed without any supports and a brim setting was provided to enable the part to print vertically (Z- direction) without falling over as seen in Figure 9. The raster angle was kept the same to ensure similar interlaminar bonding areas.

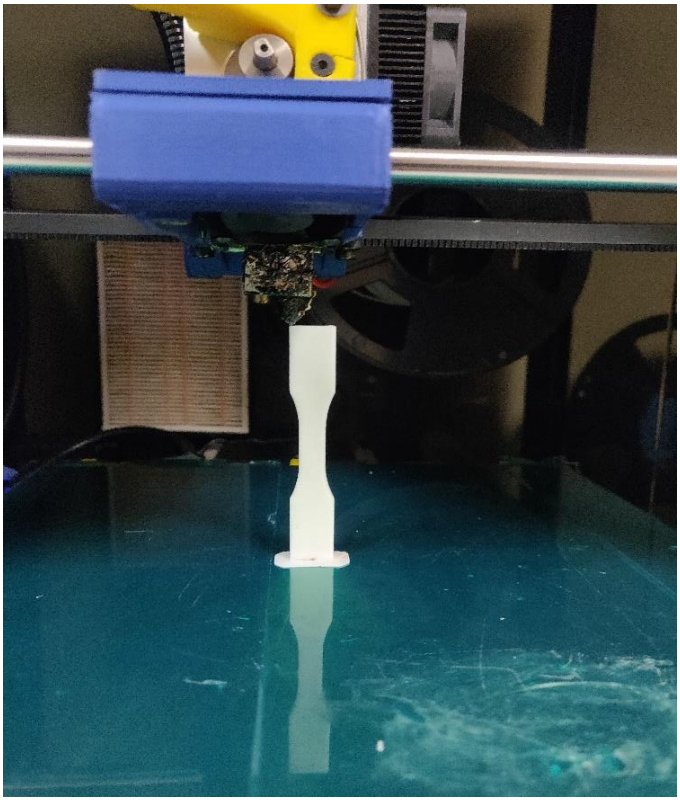

Figure 9: Printing of Dogbone specimens in Z- direction.

Each specimen was printed individually to obtain maximum interlaminar bonding and reduce the thermal gradient while printing at each layer.

3.3 Thermal Annealing and Uniaxial Pressure

Initially the dogbone specimens were heat treated by placing them in the oven for the desired time period, but substantial deformation was seen in the geometry of the parts. Thus, a custom fixture was built as seen in Figure 10, to serve the dual purpose of preventing deformation and applying a uniaxial pressure in the build direction. The fixture was made from aluminum due to its excellent conductivity thus reducing the total time required by the specimens to reach the temperature and allowing rapid cooling of the fixture.

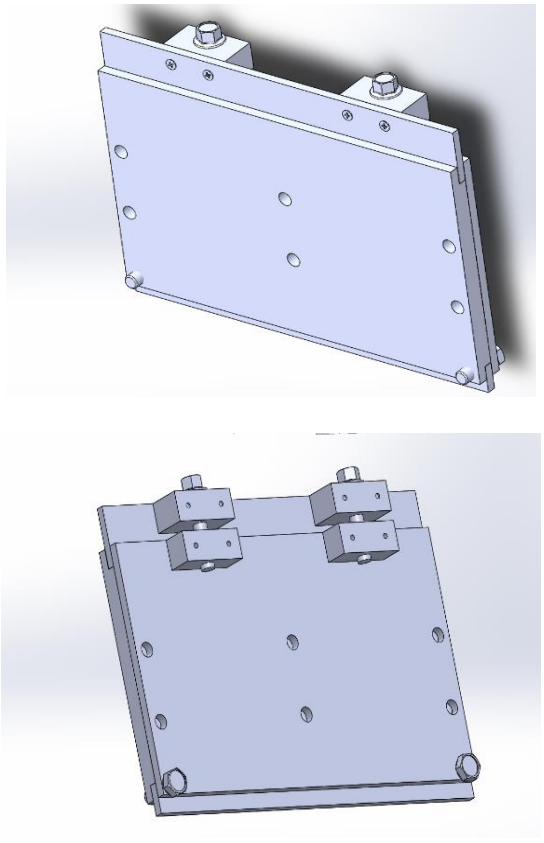

Figure 10: Custom built fixture to hold dogbones.

The fixture prevents deformation of the specimens during thermal annealing and allows for the application of a uniaxial pressure as shown in Figure 11. The pressure is applied by tightening the screws to the desired torque value using a torque wrench, this in turn causes the pressure plate to apply a uniform pressure over all the specimens in the fixture.

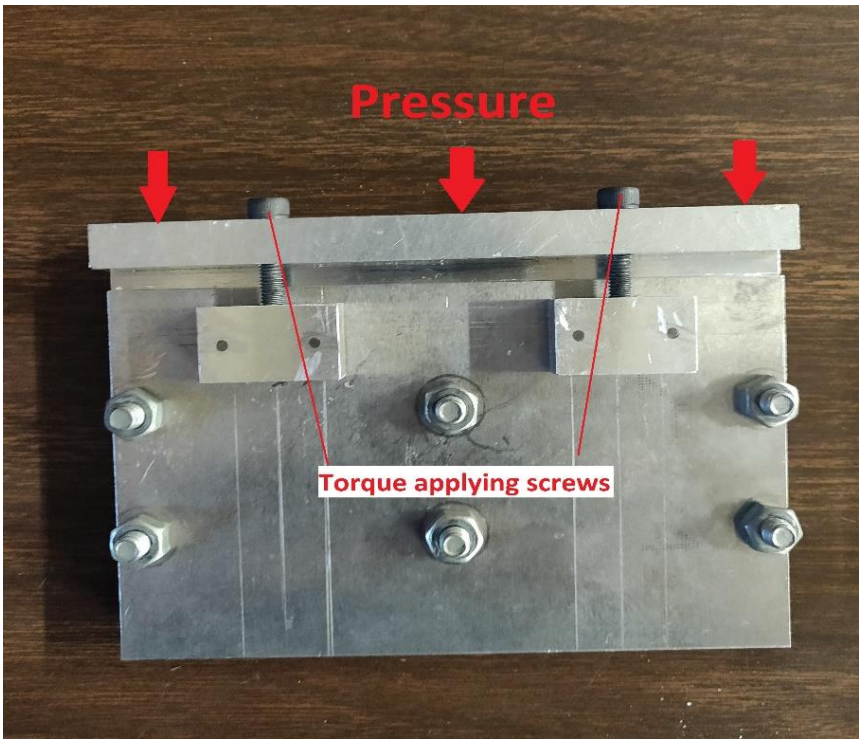

Figure 11: Uniaxial pressure being applied on the test specimens using a fixture.

Before placing the specimens in the fixture, their top and bottom ends were lightly brushed with a sandpaper to ensure identical lengths of the specimens so

that the pressure plate would have uniform contact with each specimen. To prevent the deformation of the curved portions of the specimens during the thermal annealing process, the sides of the specimens were supported using parts printed with Ultem material as seen in Figure 12. Ultem was used due to its high glass transition temperature which prevents it from fusing with ABS.

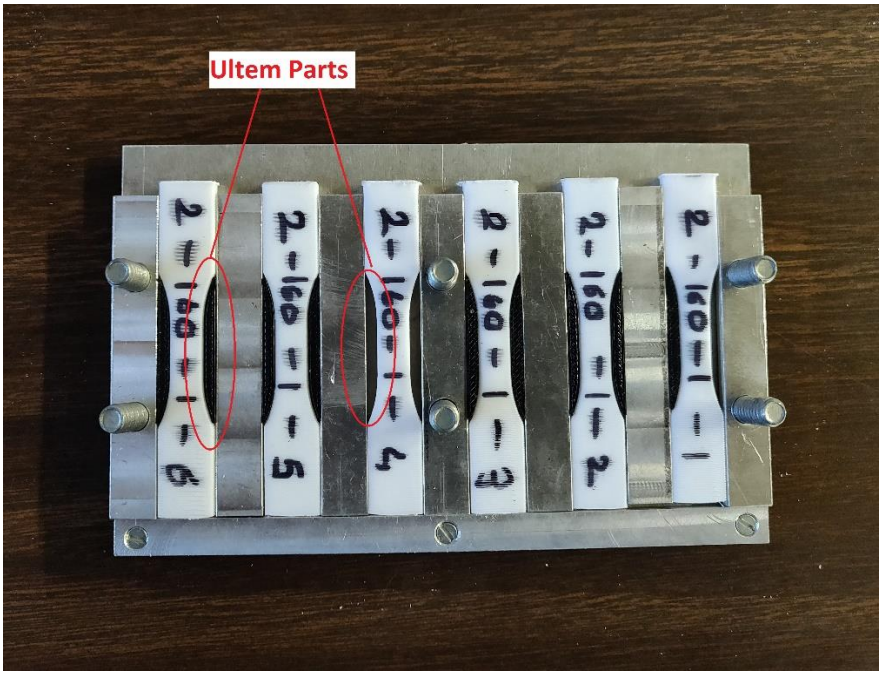

Figure 12: Ultem parts placed to prevent distortion of specimen contours.

In a previous study done by Hart et al, multiple values of temperature and times were used for thermal annealing of fracture specimens. But it is seen that as the time and temperature increase beyond a certain limit the specimens lose their geometric integrity. The goal of this work is to try and maintain the geometric

integrity of the part while increasing its tensile strength. Thus, the work done by Hart et al was taken as reference and the values of temperature and times were chosen. Hart et al had seen that the fracture toughness had increased by 400% for a thermal annealing time and temperature of 2 hours and 125°C respectively. During preliminary heat treatment tests, it was seen that for 2 hours the geometric distortion of the parts was low. Further, previous studies have suggested that though long heat treatment times lead to an increase in strength there is loss of ductility, especially for parts with low infill percentage values [26]. Thus, most of the experiments were performed for a thermal annealing time of 2 hours. In addition to the two variables, temperature and time, a uniaxial pressure was applied by tightening the screws to different values of torque. Table 2 gives the different combinations of time, temperature and pressure for the 2 sets of specimens: High print settings (Set 1) and Low print settings (Set 2).

During the heat treatment process, the oven was preheated to the desired temperature and then the fixture along with the specimens was placed inside. To check the amount of time required by the specimens to reach the oven temperature thermocouples were attached to the specimens. It was seen that the dogbones reached a steady state and were at thermal equilibrium with the oven's temperature after 1 hour. Figure 13 shows the thermocouple plots for 120°C and the approximate time required to reach steady state. Thus, a preheat time of 1 hour was

consider for each experiment and added to the total time chosen for the experiments.

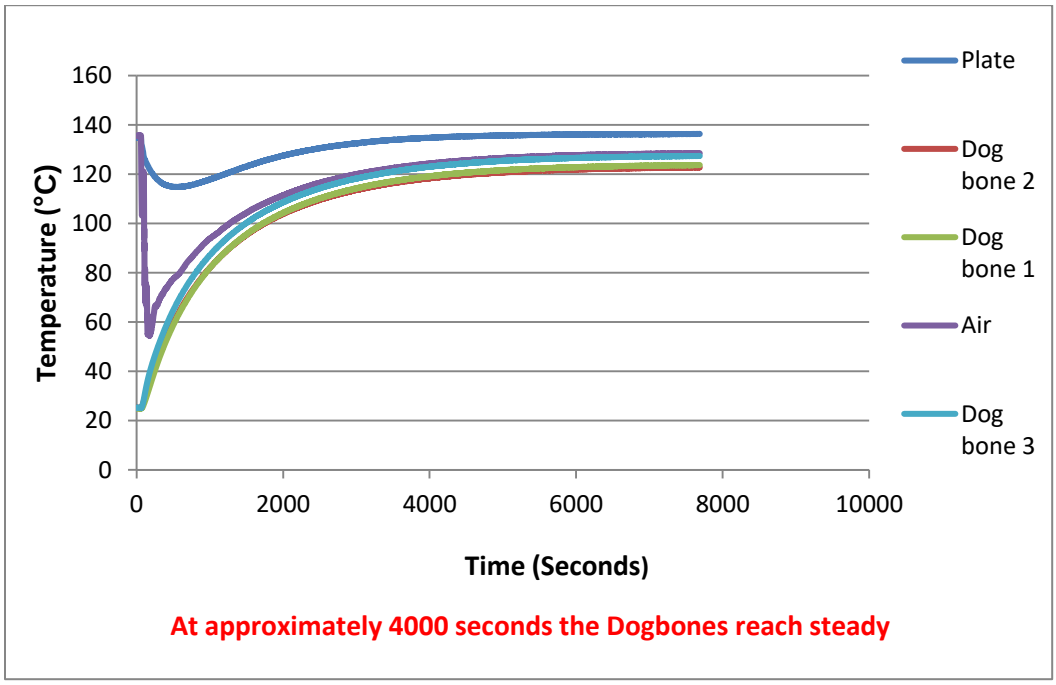

Figure 13: Thermocouple lot indicating time required to steady state.

The main differences between the two sets of specimens being tested are the extrusion multiplier, print temperature and number of perimeter shells. For the high print settings (Set 1), the values of extrusion multiplier and print temperature are set at 1.2 and 230°C respectively. Whereas for the low print settings (Set 2), the extrusion multiplier and print time are 0.8 and 220°C respectively. Previous studies have shown that using a higher value of extrusion temperature provides for better interlayer bonding [27].

Table 2: List of all the experiments performed.

Experiment Number	Total Time (Hours)	Temperature (°C)	Number of Specimens	Pressure (lb.-in)	Specimen Print Parameters
1	3	140	1	-	High
2	5	140	1	-	High
3	3	120	5	1	High
4	3	120	4	2	High
5	3	120	4	3	High
6	3	140	5	1	High
7	3	140	5	3	High
8	3	140	5	5	High
9	3	160	3	-	High
10	3	120	5	-	Low
11	3	120	5	1	Low
12	3	120	5	3	Low
13	3	120	5	5	Low
14	3	140	5	-	Low
15	3	140	5	1	Low
16	3	140	5	3	Low
17	3	140	5	5	Low
18	3	160	5	-	Low
19	3	160	5	1	Low
20	3	160	5	3	Low
21	3	160	5	5	Low
22	3	180	5	-	Low
23	1	160	5	5	Low
24	2	160	5	5	Low

3.4 Testing

The dogbones were tested under tensile loading on a Shimadzu Universal Testing Machine as seen in Figure 14. The specimens were tested using a displacement control of 5mm/min and a load cell of 1 kN was used.

Figure 14: Tensile testing of dogbone specimens

Chapter 4 Results

The tensile tests performed on the different combinations of heat treatment times, temperatures and pressure yielded data which has been grouped into various subcategories to compare the effect of different variables on the increase in strength. The subcategories have been divided based on the sets of specimens and then a comparative study has been done between the two different sets.

4.1 Characterization of Tensile Strength for Specimen Set 1

4.1.1 No Post Processing

The parts printed with higher test settings (Set 1) had an average value of maximum tensile load of 699.78 N. Table 3 shows the average values of the maximum loads before brittle failure. It is seen that the ultimate tensile strength is considerably lower than the bulk material property of ABS.

Table 3: Tensile test data of non-post processed parts (High).

	Number of Specimens Tested	Average Maximum Load (N)	Ultimate Tensile Strength of Specimen (N/mm^2)	Ultimate Tensile Strength of ABS (N/mm^2)
Set 1	4	699.78	26.45	40

Figure 15 shows the stress-strain curves of the two sets. All the plots of Set 1 specimens have a minor abnormality in the beginning section of the plot due to a loose mechanical part in the tensile test machine.

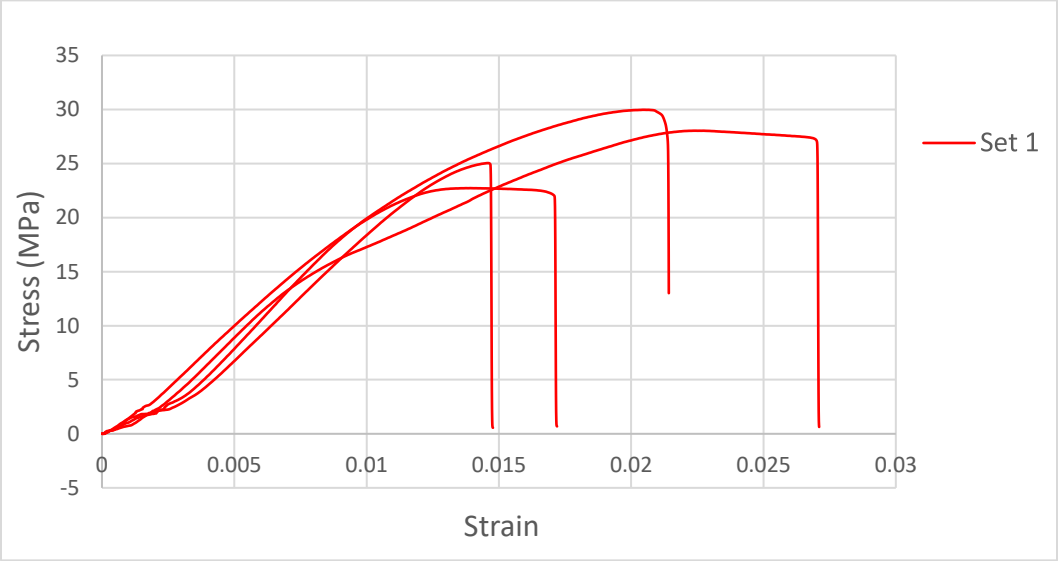

Figure 15: Stress- Strain curve for non- post processed parts.

4.1.2 Isolated Thermal Annealing

To check the effect of time, thermal annealing was done by varying the time and keeping the temperature constant. In one experiment the specimens were heated for 3 hours and 5 hours respectively while keeping the temperature constant at 140°C. In the next experiment the temperature was kept as the variable while keeping the time constant at 3 hours. The heat treatment was done for 2 different values of temperature as seen in Table 4.

Table 4: List of various combinations of temperature and time used (High settings).

Experiment Number	Temperature	Time
1	140°C	3 hours, 5 hours
2	140°C, 160°C	3 hours

Figure 16 shows the stress strain plots for the experiments with the variable time. It is seen that as time increases there is a general trend towards the increase in the ultimate tensile strength of the part. Though the increase in strength is not substantial but the parts lean towards more of a ductile failure with an increase in heat treatment time. Table 5 shows the percentage increase in ultimate tensile strength for the different heat treatment times.

Table 5: Increase in ultimate strength with time as variable (High settings)

Time	Maximum Ultimate strength (MPa)	Percentage increase in Strength
3 hours	28.19	6.57 %
5 hours	27	2.07 %

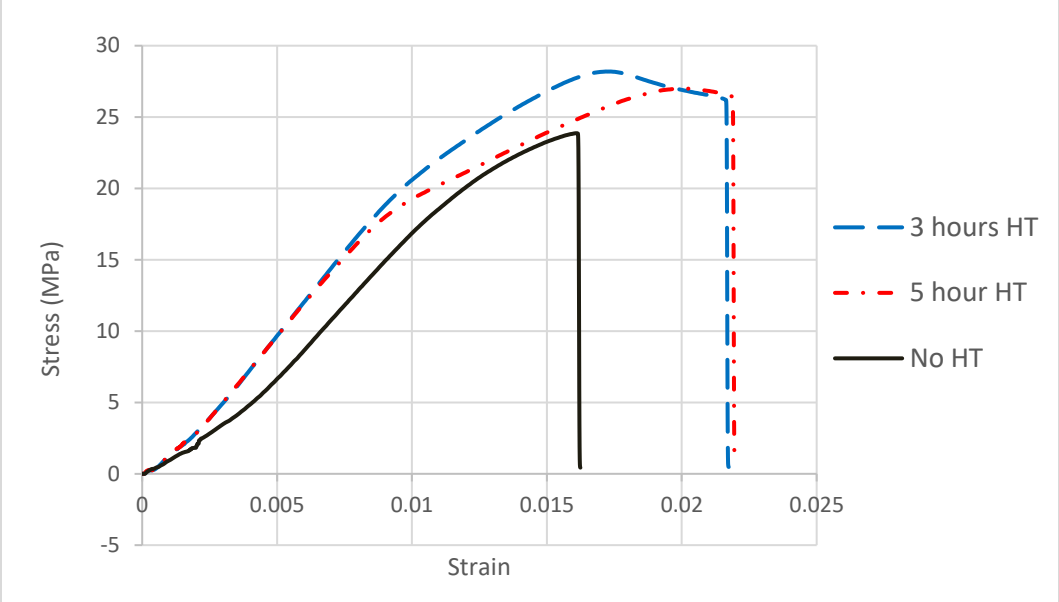

Figure 16: Stress-Strain curve for experiments with variable time (High settings)

To check the effect of temperature the specimens were thermally annealed at 140°C and 160°C. For 160°C, 3 specimens were tested, and their average ultimate tensile strength was found to be 32.75 MPa. Whereas for 140°C the maximum ultimate tensile strength was seen to be 28.19 MPa as shown in Table 6.

Table 6: Increase in ultimate strength with temperature as variable (High settings)

Temperature	Maximum Ultimate strength (MPa)	Percentage increase in Strength
140°C	28.19	6.57 %
160°C	32.75	23.82 %

Figure 17 shows the stress strain curve for the two different values of temperature. From the results obtained it is seen that an increase in temperature has a larger impact on strength as compared to thermal annealing for a larger duration of time.

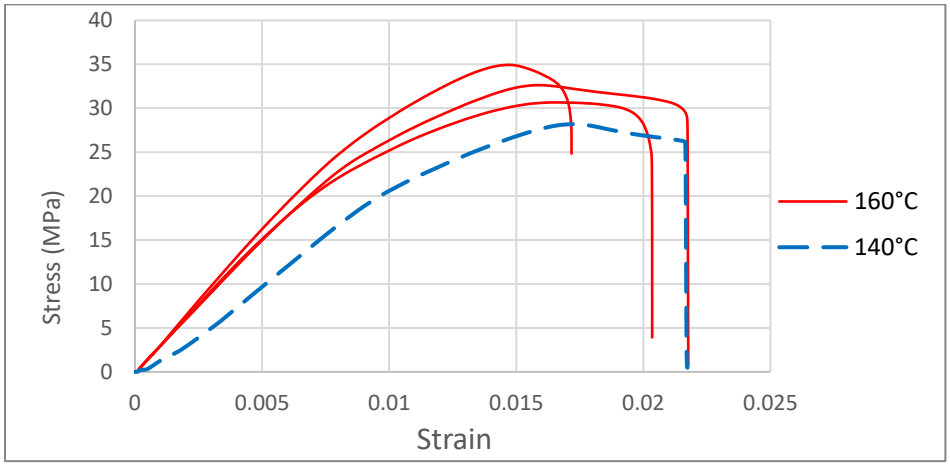

Figure 17: Stress-Strain curves for experiments with variable temperature (High settings).

4.1.3 Thermal Annealing and Uniaxial Pressure

In the mathematical models that have been developed by various authors, it is seen that intimate contact plays a role in affecting the inter-laminar strength between polymers. Uniaxial pressure was considered as a variable to try and increase the intimate contact and thus investigate its effect on increase in strength. Table 7 shows the combinations of temperatures and pressures used.

Table 7: List of various combinations of temperatures and pressures used (High settings).

Experiment Number	Temperature (°C)	Pressure (lb.-in)
1	120	1, 2, 3
2	140	1, 3, 5

For both sets of experiments, a tendency towards an increase in strength is seen with an increase in pressure as seen in Figure 20. The ultimate tensile strength spikes at the pressure value of 2 lb.-in with minor variation for all the specimens. When the pressure is further increased to 3 lb.-in a minor fall in the ultimate tensile strength is seen but a corresponding increase in modulus can be seen for most specimens. During the first set of experiments at 120°C, the tensile tests for the 1 lb.-in pressure had brittle failure with a wide variation in the ultimate tensile strength. Whereas for the other two pressure values there was a change in the slope of the stress-strain plot after a specific point indicating a change in the modulus and the failure behaved as a ductile-brittle behavior as seen in the Figure 18. It was also noticed for the pressure values of 2 lb.-in and 3 lb.-in, as the loading progressed a white zone was developed before failure occurred. This whitening of the polymer specimen can be accredited to the crazing phenomena of polymers. Crazing refers to the formation of microcracks in the polymer specimen when under tensile

loading. This is indicative of a better bond formation in the specimens at the interlaminar level.

For the second set of experiments, the temperature is increased to 140°C for the three values of pressures mentioned in Table 7. As the pressure is increased a corresponding increase in the strength is seen and a more pronounced effect on ductility is noticed. Like the first experiment, for higher values of applied pressure, crazing is noticed in the specimens before tensile failure occurs. Table 8 shows the increase in strength obtained as compared to the non-heat treated parts.

Table 8: Increase in ultimate strength with temperature and pressure as variables (High settings)

Experiment Number	Temperature (°C)	Pressure (lb.-in)	Average Ultimate tensile Strength (MPa)	Percentage Increase in Strength
1	120	1	26.74	1.09 %
2	120	2	30.02	13.5 %
3	120	3	29.71	12.32 %
4	140	1	27.09	2.42 %
5	140	3	29.71	12.33 %
6	140	5	32.47	22.76 %

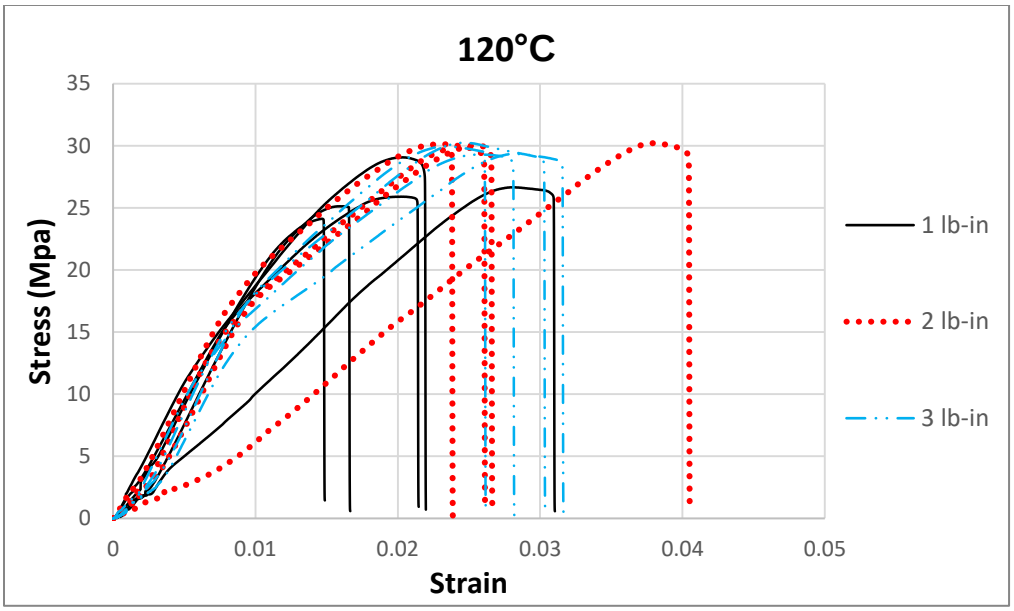

Figure 18: Stress-Strain curve for 120°C and variable pressure (High setting).

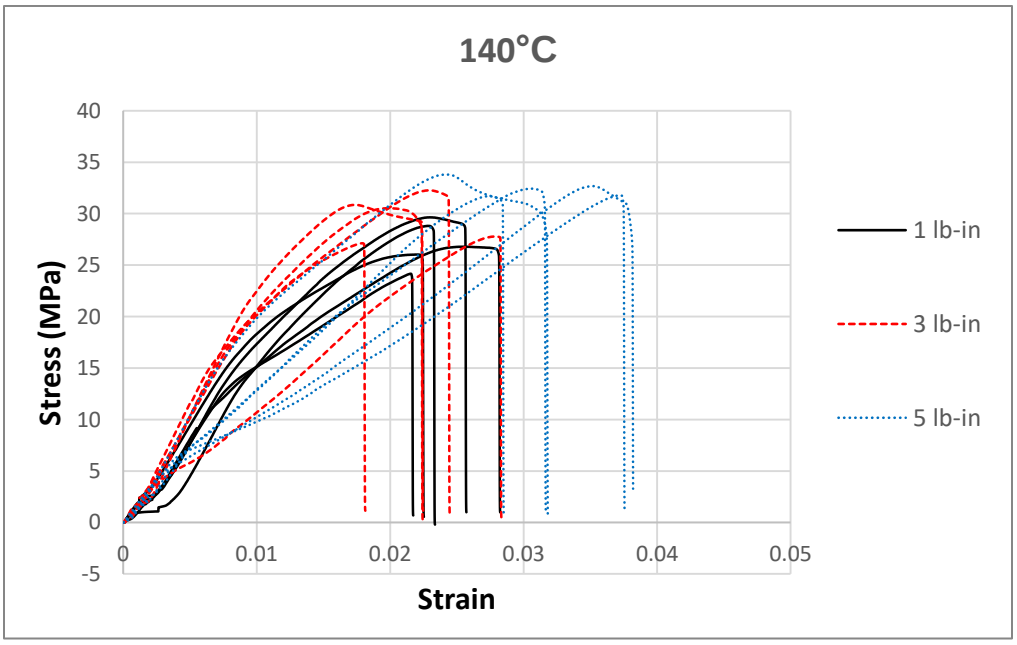

Figure 19: Stress-Strain curve for 140°C and variable pressure (High setting).

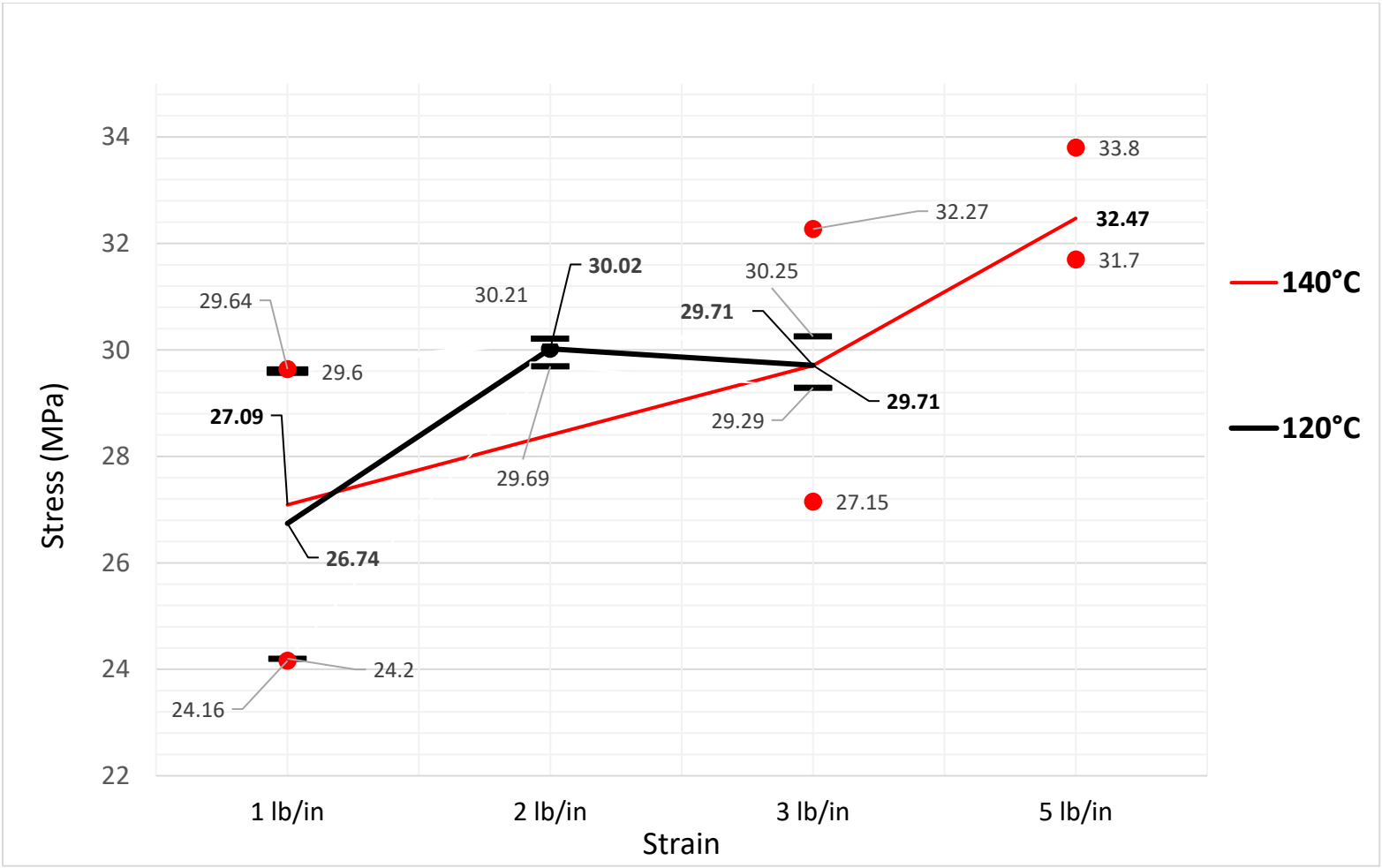

Figure 20: Comparison of ultimate tensile strength for variable values of temperature and pressure (High setting).

4.2 Characterization of Tensile Strength for Specimen Set 2

4.2.1 No Post Processing

Set 2 of the specimens were printed with low print settings and the average ultimate tensile strength is seen to be 9.677 MPa. This is considerably lower than the bulk material properties of ABS. Figure 21 represents the stress-strain curve for the tested parts, and it can be seen that all the parts undergo brittle failure.

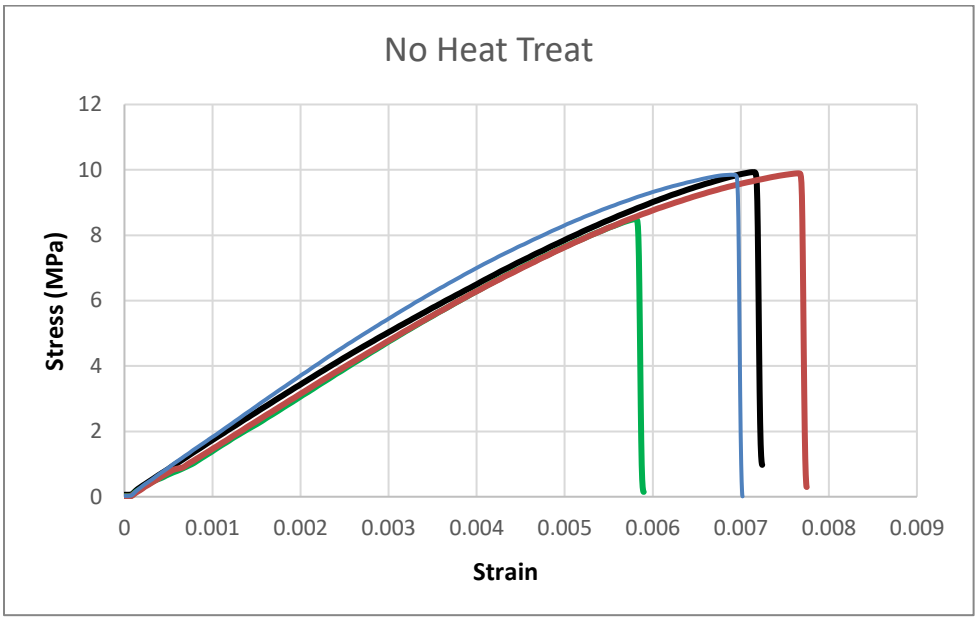

Figure 21: Stress- Strain curve for non-post processed parts (Low settings).

4.2.2 Isolated thermal annealing

For the low print settings multiple values of temperature were chosen to test its effect on the ultimate tensile strength. Table 9 shows the different temperatures used for the experiment. From Figure 22 it is seen that as the temperature goes on

increasing there is a drastic increase in the ultimate tensile strength of the specimens. For thermal annealing at 120°C it is seen that ultimate tensile strength of the parts remain almost the same as that of the non-heat treated parts. As the glass transition temperature of ABS is 105°C, thermal annealing at 120°C for 3 hours does not impart enough energy to see substantial increase in the bond length which in turn would lead to an increase in strength. But for higher values of temperature a substantial rise in strength is seen. Also, for higher values of temperature the surface finish of the parts becomes glossy and there is a reduction in the cross-sectional area of the specimens. Figure 22 shows the stress-strain relationships for the different heat treatment values. It is seen that as the temperature increases the ductility of the specimens increases along with a corresponding increase in strength and the failure shifts from a pure brittle failure to more of a ductile-brittle failure.

Table 9: List of various combinations of temperature used (Low settings).

Temperature	Time (hours)
120°C, 140°C, 160°C, 180°C	3

Figure 23 shows the cross-sectional images of the test specimens after heat treatment. For lower values of temperatures prominent voids are noticed indicating

imperfect bonding between layers. But as temperature goes on increasing the size of the voids reduces. This can be accredited to the increase in viscosity of the polymer with an increase in temperature. As the temperature is further increased the neck size or the bond length between the layers increases and at 180°C it is seen that there is almost complete bonding between layers with no visible voids. Thus, an increase in ultimate tensile strength can be seen due to an increase in the neck size and bond length between the layers.

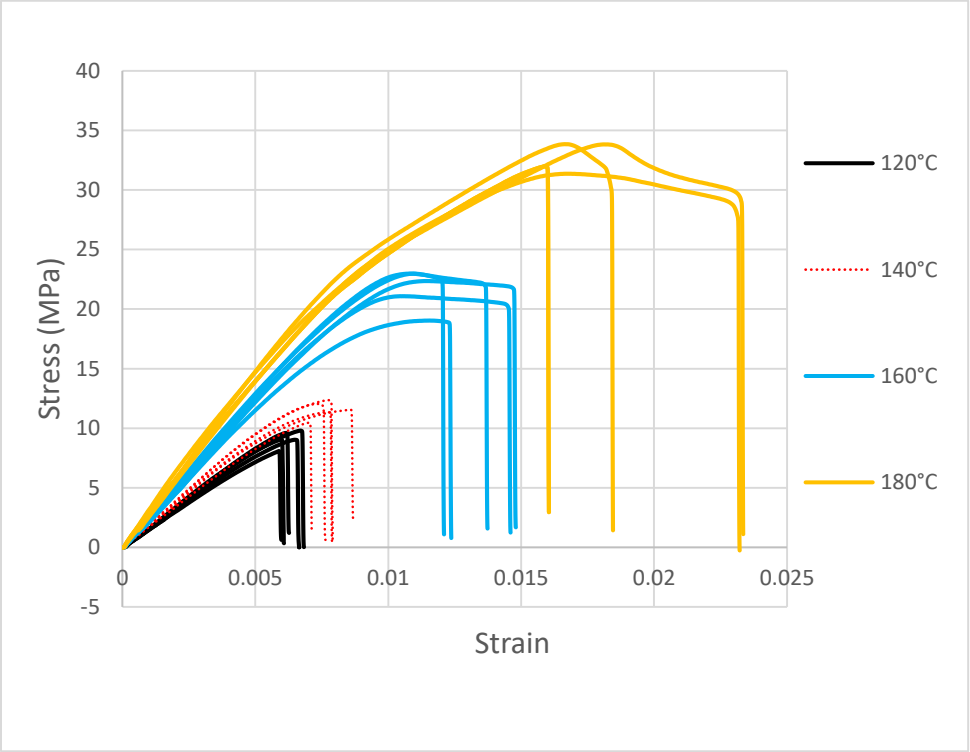

Figure 22: Stress- Strain curve for experiments with temperature variable (Low settings).

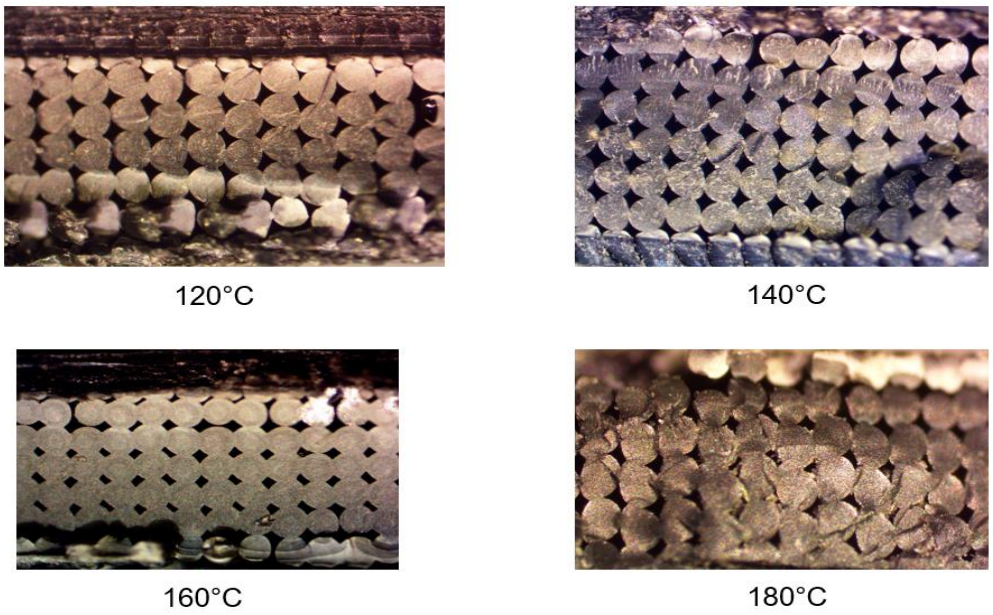

Figure 23: Cross-section of parts subjected to Isolated heat treatment (Low settings)

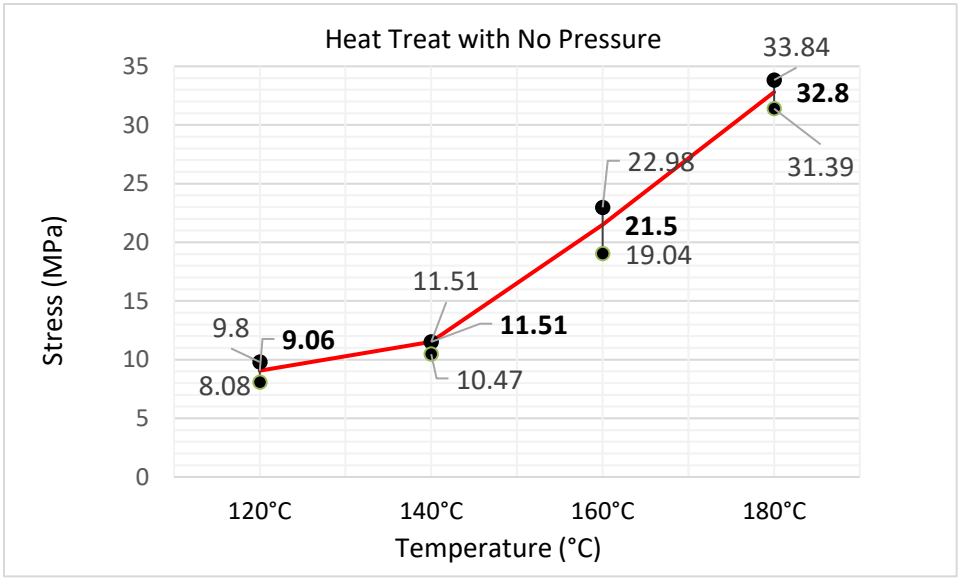

Figure 24: Plot indicating increase in Ultimate tensile strength with variable temperature. (Low settings)

Table 10: Increase in the ultimate strength for temperature as variable. (Low settings)

Experiment Number	Temperature (°C)	Average Ultimate tensile Strength (MPa)	Percentage Increase in Strength
1	120	9.06	No increase
2	140	11.51	18.94 %
3	160	21.5	122.17 %
4	180	32.8	238.94 %

Table 10 shows the percentage increase in strength of the parts corresponding to the non-heat treated parts. It is seen that after 120°C there is a steady increase in strength. This increase in strength can be correlated to the increase in bond area due to sintering at the interlaminar interfaces. The increase in temperature leads to a reduction in the size of the voids and an increase in reptation occurs across the interfaces as the polymer chains are excited.

4.2.3 Thermal Annealing and Uniaxial Pressure

To investigate the effect of pressure on the specimens printed with low settings, the dogbones were subjected to 3 different values of applied pressure for varying values of temperature. Table 11 shows the various combinations of temperatures and pressures used.

Table 11: List of various combinations of temperatures and pressures used (Low settings).

Experiment Number	Temperature (°C)	Pressure (lb.-in)
1	120	1, 3, 5
2	140	1, 3, 5
3	160	1, 3, 5

Figure 25 shows the comparative values of ultimate tensile strength obtained for all three experiments. In the first experiment (120°C), a slight increase in the ultimate tensile strength is seen. But there is wide variation in the data obtained for each value of pressure. As the magnitude of the applied pressure is increased the variation in the ultimate tensile strength goes down considerably. For the experiments at 140°C the 160°C the ultimate tensile strength peaks at the 3 lb.-in value and then falls slightly for the 5 lb.-in pressure. Overall in each experiment a rise in strength is seen with applied pressure but there is considerable variation in

the data due to the tendency of FDM parts to fail at the weakest layer due to flaws during print. The percentage increase in strength when compared to specimens thermally annealed at the same temperature but without pressure is given in Table 12.

Table 12: Increase in ultimate strength of parts with variable temperature and pressure (Low settings).

Experiment Number	Temperature (°C)	Pressure (lb.-in)	Average Ultimate tensile Strength	Coefficient of Variation	Percentage Increase in Strength
1	120	1	10.69	10.29 %	17.99 %
2	120	3	10.5	1.77 %	15.89 %
3	120	5	10.87	4.58 %	19.98 %
4	140	1	11.88	2.62 %	3.2 %
5	140	3	13.04	0.29 %	13.29 %
6	140	5	12.76	1.68 %	10.86 %
7	160	1	20.12	0.81 %	No Increase
8	160	3	22.33	1.65 %	3.8 %
9	160	5	19.97	0.36 %	No increase

From Table 12 it is seen that for 120°C and 140°C the pressure has a greater effect on increase in strength. For 160°C the strength remains somewhat constant to the values obtained for thermal annealing without any pressure, thus indicating that for higher values of temperature the applied pressure is not the controlling factor in increasing the strength.

This may be because the flow or deformation caused by the applied pressure is not as significant as the flow cause by the increase in temperature and time which leads to better sintering and void reduction in the inter-laminar regions.

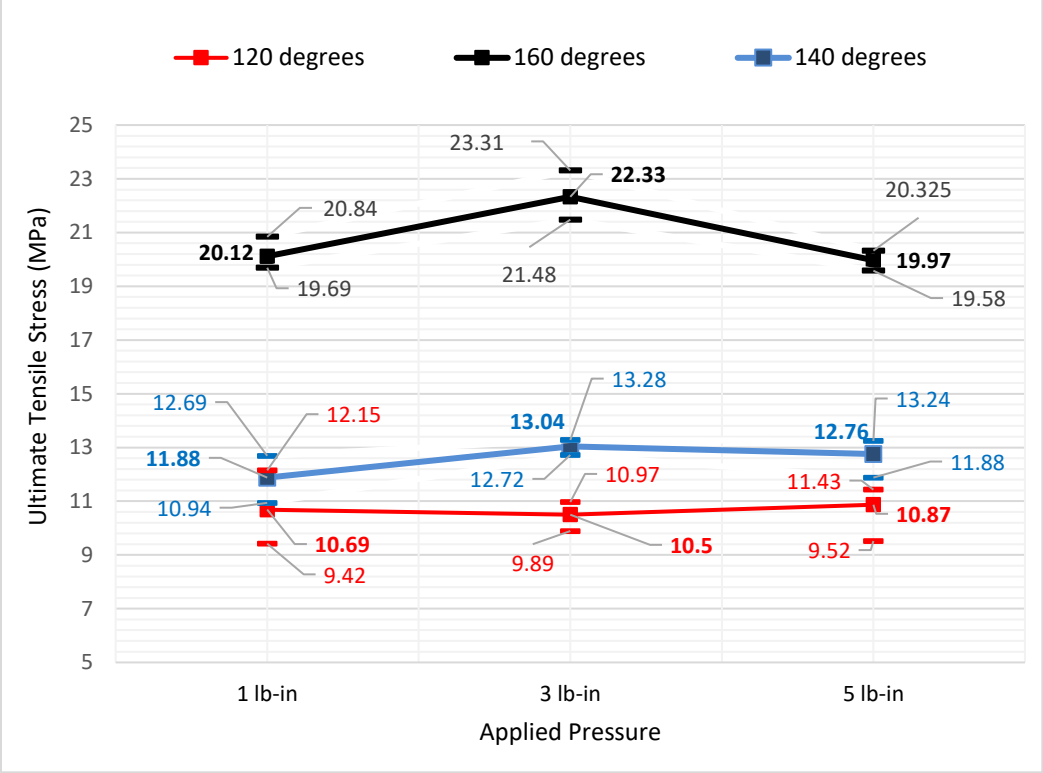

Figure 25: Comparison of ultimate tensile strength for variable values of temperature and pressure (Low setting).

4.3 Effect of Print Parameters on Strength

For the two sets of specimens printed, wide variation is seen in the strength increase even for similar post processing parameters. The non-heat treated specimens printed with higher print settings have an ultimate tensile strength which is drastically higher than the parts printed with low print settings. Though the parts printed with low settings show a considerable increase in the ultimate tensile

strength after thermal annealing, the strength is still somewhat lower than the parts printed with high print settings. This discrepancy in strength may be due to the high flow rate and larger extruder temperature used for the high print settings which lead to better material flow and sintering at the laminas. Thus, it is seen that print parameters like flow rate and extrusion temperature play a vital role in determining the bond strength of the parts printed using FDM and significantly affect their mechanical properties.

Chapter 5 Conclusion

The study was aimed to investigate the effect of isothermal annealing and uniaxial pressure on the inter-laminar tensile strength of FDM. From the study it is seen that the strength of FDM parts can be improved by using thermal annealing and uniaxial pressure. The degree of improvement in strength depends not only on the values of temperatures, times and pressures used but also on the print parameters. With an increase in the temperature and time values for heat treatment the ultimate tensile strength of the specimens goes on increasing. Accompanied with the increase in the strength an increase in the ductility of the parts is also seen.

It is seen that even for parts which are subjected to similar post processing and heat treatment parameters there is considerable variation in their ultimate tensile strength. This variation is due to the defects introduced in the individual parts during printing. The tensile specimens fail at the weakest location and it is difficult to predict the actual zone of failure due to these internal defects. Thus, the internal defects and external print conditions cause significant variability in the ultimate tensile strength of similarly post processed parts.

The cross- sectional images of the heat-treated specimens indicate a correlation between the increase in neck size and bond length with heat treatment. As the temperature is increased the bond length increases and the size of the voids decreases considerably resulting in lesser stress concentration zones. This change in the mesostructure is partially due to the increased flow properties of the polymer at higher temperatures and the reptation phenomenon occurring at the layer to layer interface resulting in better bonding.

The effect of uniaxial pressure in increasing the ultimate tensile strength is seen to be more significant for lower values of temperatures. As temperature increases the effect of pressure and intimate contact is seen to be predominated by the accentuated sintering and reptation phenomena due to higher values of temperature and time.

Though thermal annealing and uniaxial pressure cause an increase in the strength of the parts, the print parameters play a vital role in determining the initial mechanical properties of the parts. When the parts are fabricated with a higher values of flow rate and extrusion temperature, they exhibit significantly higher mechanical properties as compared to parts printed with substandard setting. Thus, by controlling the print parameters and using the right values of temperature and pressure we can see substantial increase in strength of FDM parts.

Chapter 6 Future Work

Multiple values of temperature, pressure and time have been tested in this study but there still is wide scope to understand the behavior of the interlaminar bond when subjected to the variables. To understand the effect of each variable more accurately a Design of Experiments (DOE) approach can be chosen to quantify the significance of each variable. Also, as final use parts are not just subjected to pure tension a fracture and fatigue strength analysis can be done to investigate the increase in strength. Applications such as the aerospace industry require the fabrication of complicated geometries such as the optimized thin layer aircraft wings. Though FDM provides us with the design freedom to fabricate these complex shapes, the parts so produced cannot meet with the high fatigue and fracture strength demands required in such applications. Thus, a specific combination of temperature, time and pressure while minimizing the deformation could help meet these demands.

Chapter 7 References

[1] N. Turner, R. Strong, and S. A. Gold, "A review of melt extrusion additive manufacturing processes: I. Process design and modeling," Rapid Prototyping Journal, vol. 20, pp. 192-204, 2014.

[2] H. Lipson and M. Kurman, Fabricated: The new world of 3D printing. John Wiley and Sons, 2013.

[3] Sossou, Germain. “An Additive Manufacturing Oriented Design Approach to Mechanical Assemblies.” Journal of Computational Design and Engineering, 6 Nov. 2017, www-sciencedirectcom.ezproxy.uta.edu/science/article/pii/S2288430017300659.

[4] ASTM, 2009, ASTM International Committee F42 on Additive Manufacturing Technologies, ASTM F2792–10 Standard Terminology for Additive Manufacturing Technologies, ASTM, West Conshohocken, PA.

[5] Gibson, I., Rosen, D.W. and Stucker, B. (2013), Additive Manufacturing Technologies: Rapid Prototyping to Direct Digital Manufacturing, Springer, New York, NY.

[6] Hart KR, Dunn RM, Sietins JM, Hofmeister Mock CM, Mackay ME, Wetzel ED, Increased fracture toughness of additively manufactured amorphous thermoplastics via thermal annealing, Polymer (2018), doi: 10.1016/j.polymer.2018.04.024.

[7] M. K. Agarwala, V. R. Jamalabad, N. A. Langrana, A. Safari, P. J. Whalen, and S. C. Danforth, "Emerald Article: Structural quality of parts processed by fused deposition Structural quality of parts processed by fused deposition," vol. 2, pp. 1– 15, 1996.

[8] ABS m30 [Online]. Available:(http://www.stratasys.com/materials/search/absm30)

[9] https://all3dp.com/2/infill-3d-printing-what-it-means-and-how-to-use-it/

[10] https://www.prusaprinters.org/what-are-perimeters-good-for/

[11] Forster AM. Materials Testing Standards for Additive Manufacturing of Polymer Materials: State of the Art and Standards Applicability. National Institute of Standards and Technology; 2015. May.

[12] Ziemian S, Okwara M, Ziemian CW. Tensile and fatigue behavior of layered acrylonitrile butadiene styrene. Rapid Prototyping J 2015; 21:270–8).

[13] Onwubolu GC, Rayegani F. Characterization and optimization of mechanical properties of ABS parts manufactured by the fused deposition modelling process. Int J Manuf Eng 2014; 2014:1–13.

[14] Sood AK, Ohdar RK, Mahapatra SS. Parametric appraisal of mechanical property of fused deposition modelling processed parts. Mater Des 2010; 31:287–95.

[15] Rodríguez JF, Thomas JP, Renaud JE. Mechanical behavior of acrylonitrile butadiene styrene (ABS) fused deposition materials. Experimental investigation. Rapid Prototyping J 2001; 7:148–58.

[16] Rodriguez JF. Modeling the mechanical behavior of fused deposition ABS polymer components. Notre Dame, IN: Aerospace & Mechanical Engineering Department, University of Notre Dame; 1999.

[17] Sun Q, Rizvi GM, Bellehumeur CT, Gu P. Effect of processing conditions on the bonding quality of FDM polymer filaments. Rapid Prototyping J2008; 14:72–80.

[18] K. R. Hart and E. D. Wetzel, "Fracture behavior of additively manufactured acrylonitrile butadiene styrene (ABS) materials," Engineering Fracture Mechanics, vol. 177, pp. 1-13, 2017.

[19] Rodriguez JF, Thomas JP, Renaud JE. Characterization of the mesostructure of fused-deposition acrylonitrile-butadiene-styrene materials. Rapid Prototyping J 2000;6:175–86.

[20] R.W. Messler, Jr. Joining of advanced materials; Butterworth-Heinemann (1993).

[21] Theory of Healing at a Polymer-Polymer Interface 1115 Young Hwa Kim' and Richard P. Wool*.

[22] C. Butler, R. McCullough, R. Pitchumani, and J. John Gillespie, "An Analysis of Mechanisms Governing Fusion Bonding of Thermoplastic Composites," Journal of Thermoplastic Composite Materials, vol. 11, pp. 338-363, 1998.

[23] C Ziemian, M. Sharma, S. Ziemian, (2012) Anisotropic Mechanical Properties of ABS Parts Fabricated by Fused Deposition Modeling, Mechanical Engineering, Dr. Murat Gokcek (Ed.), ISBN: 978-953-51-0505-3.

[24] Edwards, S. F. Proc. Phys. SOC., London 1967, 92,9.

[25] Doi, M.; Edwards, S. F. J. Chem. SOC., Faraday Trans. 2,1978, 1789.

[26] J. Torres, J. Cotelo, J. Karl, A.P. Gordon, Mechanical property optimization of FDM PLA in shear with multiple objectives, JOM 67 (5) (2015) 1183–1193.

[27] Aliheidari N, Christ J, Tripuraneni R, Nadimpalli S, Ameli A, "Interlayer adhesion and fracture resistance of polymers printed through melt extrusion additive manufacturing process", Materials & Design ,Volume 156, pp. 351-361, 2018.